

Contents lists available at ScienceDirect

Polymer

journal homepage: www.elsevier.com/locate/polymer



The emerging field of block copolymer self-assembly-directed quantum materials

Fei Yu^{a,b}, Ulrich Wiesner^{a,*}

ARTICLE INFO

Keywords: Block copolymer Self-assembly Quantum materials

ABSTRACT

The area of functional materials derived from block copolymers (BCPs) as structure-directing agents for various inorganic materials has seen substantial growth as a result of the immense scientific as well as technological promise associated with such hybrid materials. The convergence of BCP self-assembly with the fast-growing field of quantum materials now promises solution-based synthetic approaches to classes of materials that to date are dominated by stringent high-vacuum physical deposition techniques and bulk solid state chemical reactions. Moreover, the ensuing periodic nano- and mesostructures, a characteristic of BCP self-assembly, offer a unique platform for manipulating quantum-level properties, in turn resulting in substantial changes of macroscopic properties. This article will make a case for, review the existing work of, and provide our perspectives on this emerging field of block copolymer self-assembly directed quantum materials.

1. Introduction & motivation

Despite their revolutionizing impact on human civilization, polymer materials typically suffer from limited electrical, magnetic [1], and photonic [2] functionalities. Creating composites by simply mixing in inorganic components with desired properties expands the scope of property profiles and associated applications, but oftentimes with only limited control over periodically ordered nano- or mesostructures. Due to the unfavorable interaction between different chemical blocks, block copolymers (BCPs) spontaneously (self-)assemble into an array of periodically ordered structures on the mesoscale [3]. To address the lack of functionalities associated with pure organic polymeric components, precursors to inorganic materials or inorganic nanoparticles can be added to preferentially swell specific blocks of BCPs [4,5]. Together, they undergo cooperative assembly, e.g., via solvent evaporation induced self-assembly (EISA), to produce a similar array of mesophases [6]. The use of BCPs as a structure-directing agent introduces well-defined periodic mesostructures to the functional inorganic materials, including carbons [7,8], ceramics [6,9], semiconductors [10], metals [11], and metal oxides [12,13]. Furthermore, pyrolysis of the resulting mesostructured composites leads to mesoporous solids useful for a wide range of applications from separations, energy conversion and storage, all the way to catalysis and photocatalysis [14].

In addition to the mesostructural control over conventional inorganic materials, Wiesner et al. have recently reviewed the convergence of soft matter and quantum materials [15]. A broadly defined umbrella term in condensed matter physics, quantum materials refer to materials with their properties established and described by high-level quantum mechanics, with no counterparts in (semi-)classical mechanics [16]. Examples of quantum materials include superconductors [17], topological insulators [18], and spin ices/liquids [19,20]. In recent years, these materials with often exotic properties have emerged as an exciting topic galvanizing the scientific community as well as the public, fueled by progress in quantum computing and associated quantum information technologies [21,22]. However, to date this topic has largely been dominated by the solid-state physics community, with very little overlap with the soft matter community. In part this is due to the very different educational backgrounds of these communities and emphasis on different methodologies and approaches to materials formation and their studies.

As we argued recently, however, "there is plenty of space in the middle", with substantial academic as well as technological promise of soft matter enabled quantum materials [15]. Having a built-in superlattice on the mesoscale, i.e., beyond the length scale of the atomic unit cell, is known to induce surprising materials behavior, as exemplified by the superconductivity of magic-angle graphene [23]. The self-assembly

E-mail address: ubw1@cornell.edu (U. Wiesner).

^a Department of Materials Science and Engineering, Cornell University, Ithaca, NY, 14853, USA

b Department of Chemistry and Chemical Biology, Cornell University, Ithaca, NY, 14853, USA

^{*} Corresponding author.

of soft matter offers rich and versatile bottom-up pathways to generate periodic nano- and mesoscale structures with lattice parameters at the hundreds of angstroms scale. This leads to potential coupling with atomic level phenomena, e.g., through the confinement of charge carriers in the limited space defined by the building blocks of the superlattice. Furthermore, unexpected results may emerge and open up quests for understanding of underlying new physical phenomena. Therefore, the crossover between condensed matter physics and soft matter science is a rich playground for academic studies. Moreover, the utilization of soft matter, amenable to solution processing, dramatically facilitates processing approaches with improved scalability and reduced costs relative to traditional methods. For example, materials fabrication may no longer be restricted by high vacuum techniques, which has dominated a range of physical deposition methods, e.g., molecular beam epitaxy (MBE) [24], pulsed laser deposition (PLD) [25], or various sputtering methods, and is the current quantum materials synthesis paradigm. Moving to solution based soft matter approaches provides access to a diverse set of form factors beyond thin films that can be explored. This potentially includes additive manufacturing (also known as 3D printing) [26], enabling rapid lab-scale proof of concept, commercial design prototyping, or large-scale industrial manufacturing. These academic as well as technological merits, together, make a strong case for increased research efforts into soft-matter self-assembly based quantum materials.

This article will focus on reviewing recent work, primarily from the Wiesner research group at Cornell University, on BCP self-assembly directed quantum materials. It will be demonstrated how BCPs can access a diverse range of morphologies, e.g., of superconductors, on multiple length scales by tuning molar mass [27], block ratios [3] and architectural designs (Fig. 1) [28]. As with other polymers, in general BCPs can be adapted to a plethora of processing conditions such as solution-based spin-coating and roll-to-roll processing, or melt-based injection molding and extrusion, resulting in a range of form factors such as particles, thin films, and bulk materials. A few examples of these processing approaches that have already been realized will be described.

The article will highlight how, employing BCPs as structure directing agents for various inorganic material precursors or nanoparticles, superconductors (Section 2) and other types of quantum materials (Section 3) with unique periodic mesostructures and network topologies can be derived. Emphasis will be on demonstrating that, by changing fundamental quantum materials characteristics, such periodic lattices substantially alter the macroscopic properties of the resulting quantum materials relative to the bulk, resulting in quantum metamaterials. In the final part of the review, critical perspectives are provided in Section 4 on future opportunities as well as challenges associated with this emerging research field.

2. BCP self-assembly-directed superconductors

2.1. Monolithic gyroidal mesoporous superconductors

Phenomenologically, electrical resistance vanishes in superconductors (Fig. 1, upper right) below the critical temperature (T_c). The combination of polymers with superconductors in a composite was reported in the early 1990s [29] as an attempt to solve the problem of mechanical brittleness associated with many high- T_c superconductors. However, there has been scant research effort that leverages the self-assembly power of BCPs to create well-defined periodically ordered nanostructures for the study of the interplay between mesostructure and superconducting properties. This synthetic task is non-trivial. Many superconductors are metals above T_c . Forming, e.g., continuously connected nanostructures of metals via BCP self-assembly has been a considerable challenge in the polymer community [11,30,31]. Furthermore, the highly curved interfaces in a number of self-assembled mesostructures (vide infra) are expected to lead to large-angle grain boundaries in the crystalline phase of the inorganic materials. For anisotropic crystal structures of superconductors, e.g., the tetragonal lattice of yttrium barium copper oxide (YBa2Cu3O7-x, YBCO), charge carrier transport across such grain boundaries is substantially reduced, leading to low quality macroscopic property profiles. As alluded to in the

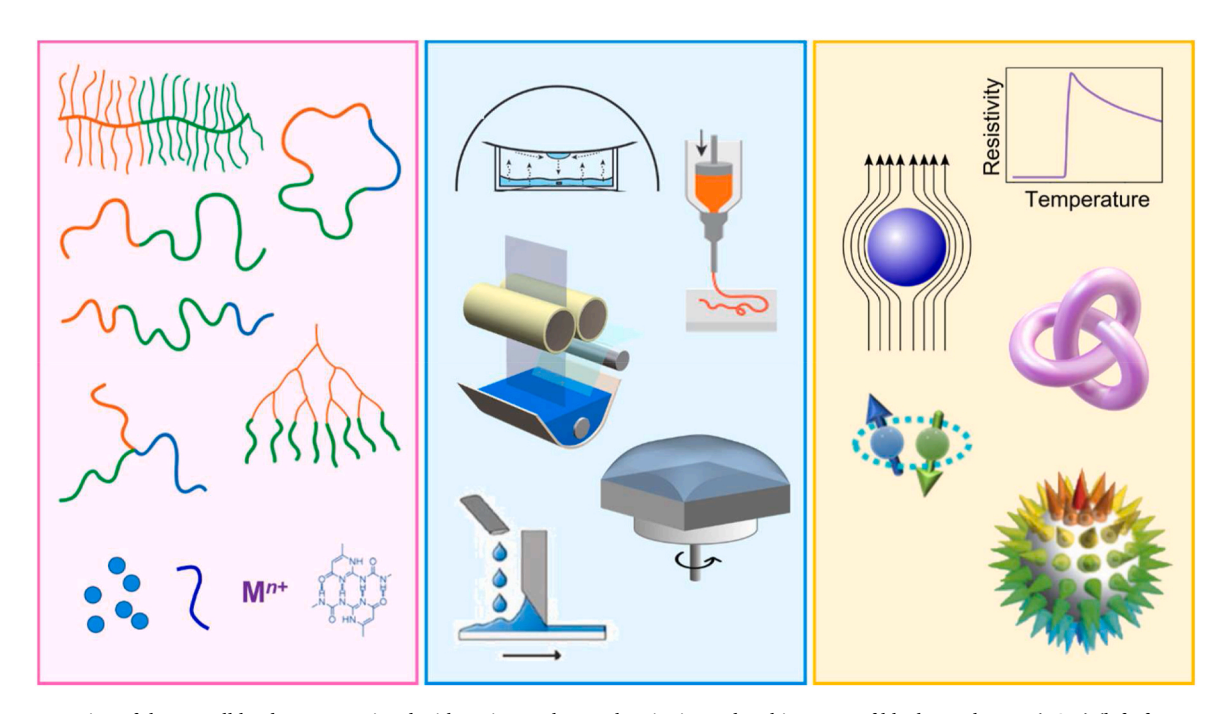


Fig. 1. Representation of the overall landscape associated with various polymer chemistries and architectures of block copolymers (BCPs) (left, from top to bottom: BCP brushes, BCP rings, diblock and triblock polymers, dendritic BCPs, BCP stars, nanoparticles, homopolymers, metal cations, and hydrogen bonding units), solution processing methods (middle, from top to bottom: evaporation-induce self-assembly (EISA), roll-to-roll, spin-coating or doctor blading) and different quantum materials (right, from top to bottom: temperature dependent resistivity of a superconductor exhibiting zero resistance, schematic of magnetic field expulsion by a superconductor (Meissner effect), graphic representation of topological entanglements, fermion pairing in a Cooper pair, and structural representation of a magnetic skyrmion).

previous section, however, the dual scientific and technological promise of such BCP self-assembly-directed quantum materials called for development of bottom-up synthetic routes that would overcome these challenges.

Versatile schemes exist involving amphiphilic BCPs as structure-directing agents for metal oxides via sol-gel routes [5,12,13,32]. Metal oxide sols obtained from hydrolysis of metal precursors (such as metal alkoxides or metal halides) can preferentially mix with the hydrophilic block of amphiphilic BCPs. Upon solvent evaporation, a combination of self-assembly and sol-gel transition then forms the desired BCP-metal oxide hybrid mesostructures [5,6]. Hybrids can subsequently be translated into mesoporous metal oxides via removal of organic/polymeric components, e.g., by thermal decomposition.

Once mesoporous metal oxides are obtained from BCP self-assembly, it becomes possible to convert them into superconductors via solid state chemical reactions. In the first example of a BCP self-assembly directed mesostructured superconductor (Fig. 2) [33], niobium oxide sol-nanoparticles were first structure-directed into a co-continuous alternating gyroid (G^A) morphology (Fig. 2a) using triblock terpolymer poly(isoprene-block-styrene-block-ethylene oxide) (PI-b-PS-b-PEO, or ISO) as structure directing agent. The resulting hybrid

was subsequently heat treated in air to generate amorphous (Fig. 2f) niobium pentoxide (Nb2O5). The oxide was finally heat treated in ammonia (NH₃) in two steps to arrive at superconducting niobium nitride (NbN), an extensively studied type-II superconductor with applications, e.g., as Josephson junction-based voltage standards and commercial use for single photon counting important in astronomy and telecommunications [34–36]. Of the common phases of NbN, δ -NbN has a cubic (rock salt) atomic lattice. It therefore was expected that large-angle grain boundaries between NbN crystal grains anticipated to occur when filling the curved co-continuous minority volumes of a GA structure would not diminish electronic transport across bulk samples (vide supra). In the co-continuous G^A network structure of the as-made material, the niobia sol selectively swelled the hydrophilic PEO block, forming one of the two interpenetrating minority networks of the gyroid structure (green volume in structural schematic in Fig. 2a). The second minority network (blue volume in structural schematic in Fig. 2a) as well as the majority volume (open volume between the two minority networks in Fig. 2a) occupied by PI and PS blocks, respectively, were removed during calcination in air. This left behind a highly porous co-continuous minority network structure as characterized by scanning electron microscopy (SEM, Fig. 2b-d). The GA morphology was retained

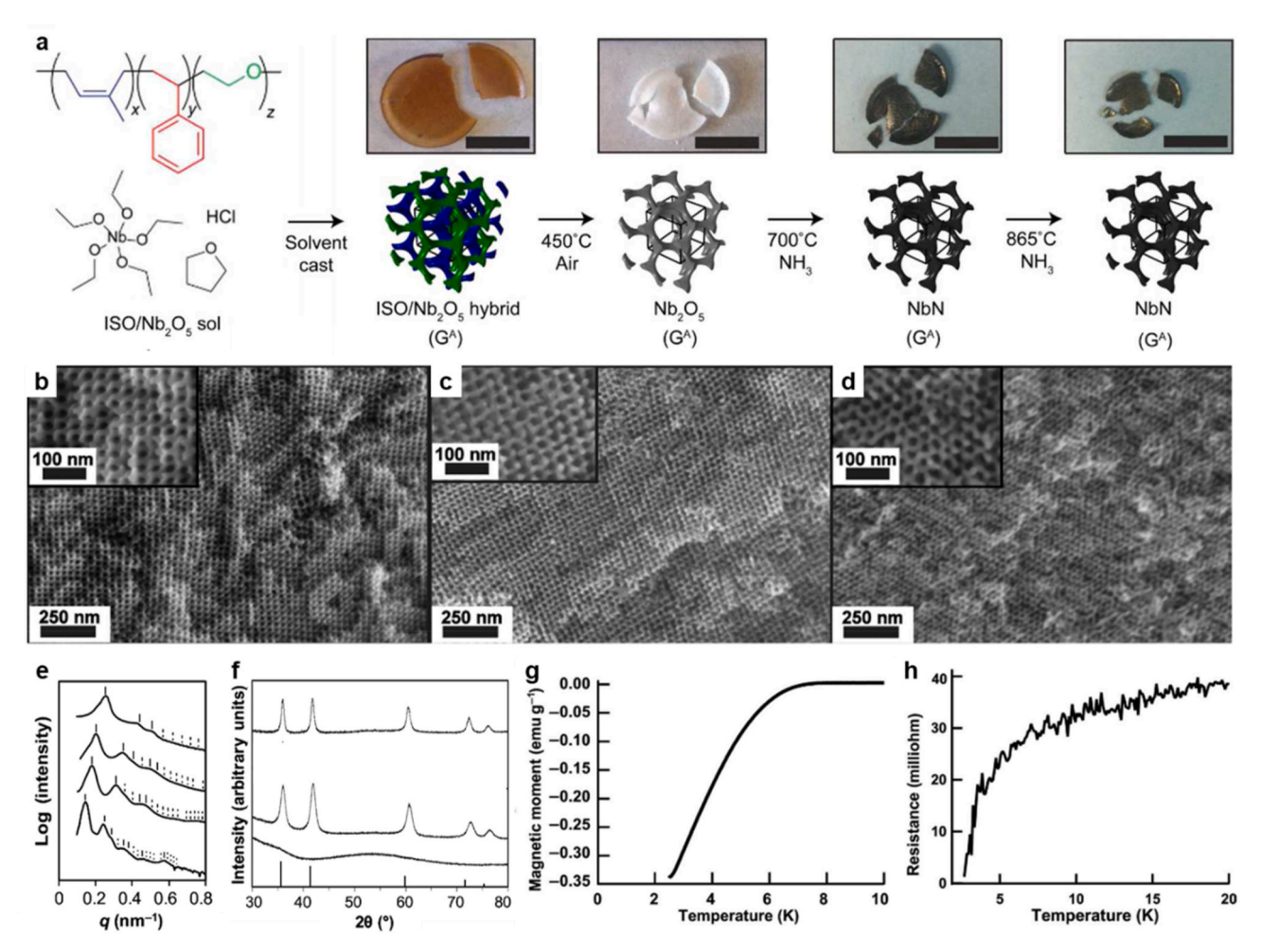


Fig. 2. (a) Schematic of the procedure to prepare mesoporous NbN superconductors with alternating gyroid (G^A) morphology via self-assembly of poly(isoprene-block-ethylene oxide) (ISO) and Nb₂O₅ sol nanoparticles and subsequent heat treatments. Photographs above show materials at the corresponding processing step (scale bar represents 1 cm). Scanning electron microscopy (SEM) images of mesoporous (b) Nb₂O₅ and NbN after heating in NH₃ at (c) 700 °C and (d) 865 °C. (e) Small-angle X-ray scattering (SAXS) profiles of (from bottom to top) ISO–Nb₂O₅ as-made hybrid, amorphous Nb₂O₅, and NbN after 700 °C and 865 °C treatments in NH₃, respectively. Ticks indicate expected peak positions for a G^A lattice. (f) Powder X-ray diffraction (XRD) profiles of (from bottom to top) amorphous Nb₂O₅, and crystalline NbN after 700 °C and 865 °C treatments in NH₃, respectively. Ticks indicate expected peak positions and relative peak intensities for a cubic rock salt NbN from powder diffraction file (PDF) 04-008-5125. Plots of (g) magnetic moment measured by a vibrating-sample magnetometer (VSM) and (h) electrical resistance as a function of temperature in a range covering the critical temperature (T_c) for mesoporous NbN. Adapted from Ref. [33] with permission from American Association for the Advancement of Science.

across all thermal processing, i.e., also after the final heating step in ammonia at 865 °C. The GA lattice shrank substantially (almost by a factor of two) during these thermal treatments at higher temperatures, as revealed by the Bragg reflections shifting to higher momentum transfer (q) in small-angle X-ray scattering patterns (SAXS, Fig. 2e). The atomic crystal structure was consistent with cubic rock salt NbN as revealed by X-ray diffraction (XRD, Fig. 2f) and showed a grain size of 13.6 nm (as determined from the coherently scattering domain size via Scherrer analysis), smaller than the mesostructural minority network strut width of 15.2 nm. Key to successful mesostructured superconductor formation was to strike a delicate balance between achieving sufficient nitridation while preserving mesostructural integrity: While a high enough quality nitride crystal structure critical for reaching the superconducting state was achieved by moving to relatively high nitridation temperatures (especially in the second higher and shorter heat treatment under ammonia), mesostructural integrity was ensured by (1) using a niobia sol with particle sizes smaller than the radius of gyration (R_{σ}) of the PEO block [37], and (2) heat treatment protocols with optimized temperature ramps for oxidation and nitridation to, respectively, (i) allow for an amorphous Nb₂O₅ to crystalline NbN transition (rather than a more disruptive crystal-crystal transition between these two phases) and (ii) prevent NbN crystal overgrowth beyond the confines of the

A superconductor is typically characterized by two properties at temperatures below T_c : (1) vanishing electrical resistance, and (2) expulsion of external magnetic fields (known as the Meissner effect, Fig. 1 [38]). The latter Meissner effect is manifested as a negative magnetic moment (opposing the externally applied magnetic field) developing as the sample is cooled below T_c . For the BCP self-assembly directed mesoporous NbN, low-temperature electrical transport measurements and vibrating sample magnetometry, the latter to capture the materials magnetic response, unambiguously established superconductivity of samples with a T_c of 7-8 K (Fig. 2g and h). Compared with state-of-the-art bulk NbN with a T_c around 16 K [39], however, the lower T_c observed for BCP self-assembly-directed NbN suggested lower quality materials possibly due to chemical or physical impurities, non-stoichiometry, or inherent nanoscale feature sizes [40,41]. Impurities, including residues as a result of incomplete calcination of organic components and the furnace heat treatment environment, engender severe scattering of charge carriers leading to so-called "dirty" superconductors [42]. Non-stoichiometry caused by the presence of vacancies and oxygen, as evidenced by the intermediate atomic crystal lattice sizes between pure cubic NbN and niobium oxide (NbO), likely also contributed to scattering. In fact, only around 30% of magnetic flux was expelled at 2.5 K based on the initial change of field-dependent magnetic moment (or 5% if a reference of dense bulk NbN was used [33]), indicating a large fraction of non-superconducting components. All this suggested that improved approaches to these BCP directed superconductors were required to be able to generate materials competitive with those obtained from traditional fabrication methods.

2.2. Superconducting quantum metamaterials

An important fundamental insight on the way to high-quality BCP solution-based superconducting NbN came from a subsequent study by the Wiesner group on these materials [43]. Because of the mesoporous nature of the oxide coupled with small wall thickness (typically 10–20 nm for BCPs of 50–150 kg/mol molar mass) and associated short diffusion length relative to the bulk, the conversion from oxide to nitride under ammonia readily occurs at temperatures well below 1000 °C, i.e., far below NbN's melting temperature (2573 °C). As a result, high-quality mesostructured nitrides can be formed via the following two-step thermal treatment approach: In a first heating step, e.g., up to 700 °C under ammonia, the amorphous mesoporous oxide is converted to a crystalline nitride via reactive precipitation in the oxide phase. The temperature of this heating step determines the size of the precipitated NbN crystals.

This is followed by a second heating step under either inert (e.g., argon), reducing/forming (H₂/N₂), or carburizing (CH₄/H₂/N₂) atmosphere to temperatures as high as 1000 °C, where the atomic crystal quality of the nitride (or carbonitride in case of carburizing gas) is improved, but very little to no Oswald ripening of these crystals takes place, preserving the BCP directed mesoporous nanostructure (Oswald ripening is typically suppressed at temperatures lower than half the material's melting temperature). Using this insight, the crystal lattice size increased from 4.32 Å using the previous protocol of annealing under NH₃ up to 865 °C to 4.42 Å after thermal treatment under carburizing gas up to 1000 °C (determined from X-ray diffraction, XRD), closer to the bulk value of 4.45 Å (Fig. 3a). As determined from the onset temperatures of repulsion of magnetic flux by the superconductor, the trend of increasing T_c in response to improved thermal treatments in different gases was in agreement with increasing crystal lattice parameters. The sample annealed in carburizing gas up to 1000 °C showed a T_c of 16.0 K (Fig. 3b), a marked increase by a factor of two from the original value of 7-8 K and consistent with state-of-the-art materials (vide supra). Additionally, a stronger diamagnetic response to applied external magnetic fields demonstrated a higher percentage of superconducting material.

The same study also demonstrated that NbN superconductors structure directed by BCP self-assembly into different periodically ordered porous mesostructures show different superconducting properties, despite almost identical atomic lattice constants. These materials were therefore referred to as BCP directed superconducting quantum metamaterials. The tunability of BCP self-assembly was exemplified when different morphologies were generated by progressively adding into the synthesis mixture more niobia sol relative to the same amount of parent ISO triblock terpolymer (Fig. 3c). After identical processing employing optimized thermal processing conditions up to 1000 °C in carburizing gas, periodically ordered mesoporous NbCN with GA, perforated lamellae, double gyroid (GD), and hexagonally packed cylinder morphologies (in the order of increasing niobia sol content, Fig. 3f-m) displayed increasing Tc's (Fig. 3d), while their XRD patterns, revealing the corresponding atomic lattices typically dictating quantum behavior, were essentially indistinguishable (Fig. 3e). While the origin of this metamaterial behavior remained unclear and required further studies, these results suggested that the highly tunable chemistries, compositions, length scales, and mesostructures of BCPs provide a powerful platform for the future design of soft matter enabled quantum materials.

An alternative pathway toward mesostructured metals that turn into superconductors at low temperatures is to backfill metals directly into a periodically ordered mesoporous template already made through BCP self-assembly. This multistep templating strategy differs from the aforementioned structure-directing role played by BCPs. While involving more steps, it allows a greater degree of freedom in terms of materials choice as BCP and metal chemistries don't have to be compatible. Furthermore, this more modular synthesis approach decouples materials chemistry and composition from mesostructured materials formation. The resulting mesostructured metals superconductors confined in the template can be juxtaposed and directly compared with their bulk counterparts, e.g., in terms of their superconducting properties, without concerns for significant changes in composition that are introduced, e.g., during heat processing steps in samples prepared via the structure direction pathway. To facilitate conformal and complete backfilling, a template with a 3D co-continuous network morphology is preferred. To that end, a G^D was self-assembled from triblock terpolymer poly(isoprene-block-styrene-block-dimethylaminoethyl methacrylate) (PI-b-PS-b-PDMAEMA, or ISA) mixed with preceramic polymer polymethylvinyl silazane (PMVS, trade name Durazane 1800) [44,45]. During calcination and heating in ammonia, the two minority core-shell gyroidal networks composed of PI cores and PS shells were removed while the majority matrix material (PMAEMA block + PMVS) turned into a chemically robust and mechanically strong silicon oxynitride (SiON). Monoliths of the resulting SiON with empty 3D double gyroidal minority network pore spaces now can serve as a

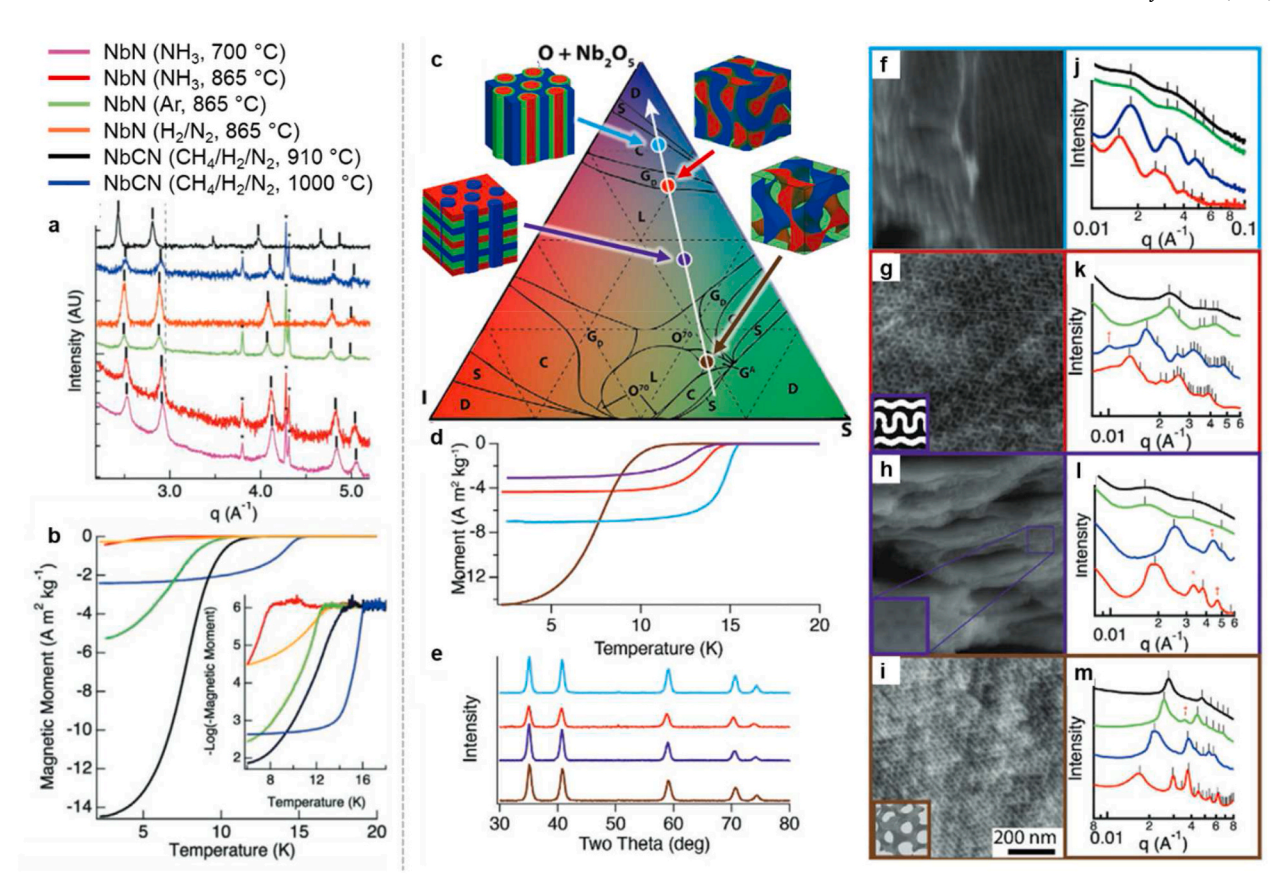


Fig. 3. (a) XRD profiles and (b) temperature-dependent magnetic moments of BCP self-assembly directed monolithic mesoporous NbN or niobium carbonitride (NbCN) samples annealed in different gases and temperatures (see legend at the top), starting with the same NbN nitridized at 700 °C. The inset of (b) presents magnetic moments in logarithmic form facilitating determination of T_c . Note that the black and blue curves in (b) should be switched (this is an error in the original publication). (c) Illustrative ternary phase diagram of the ISO-terpolymer system showing the isopleth (white arrow) along which a series of different morphologies are expected by incorporating more niobia sol to the starting parent ISO, thereby effectively swelling the PEO block volume fraction only. (d) Temperature-dependent magnetic moments and (e) XRD profiles for mesoporous NbCN with different morphologies. (f–i) SEM images of corresponding NbCN after 1000 °C treatment in carburizing gas. Insets in (g–i) show simulated projections of the respective mesophases in agreement with SEM observations. (j–m) SAXS profiles of corresponding mesophases at different processing stages. In each panel, the SAXS curves correspond to (from bottom to top) ISO-Nb2O5 as-made hybrid (red), mesoporous Nb2O5 (blue), mesoporous NbN (green), and mesoporous NbCN (black). Ticks indicate expected peak positions for corresponding mesostructural lattices (i.e., from j to m: core-shell hexagonally packed cylinders, core-shell double gyroids (G^D), perforated lamellae, and G^A). Note the different color schemes for each: (a,b), (c–m), and within the boxes of (j–m). Adapted from Ref. [43] with permission. © 2021 Wiley-VCH.

mesoscale mold for the backfilling with appropriate metals, including those which otherwise are challenging to be fashioned into periodically ordered mesostructures.

Indium (In) with a low melting point of 157 $^{\circ}\text{C}$ was chosen as a type-I superconducting metal and backfilled into the mesopores of the G^D SiON template via high (400 MPa) pressure infiltration at 250 °C (Fig. 4a) [46]. SEM (Fig. 4b) and energy-dispersive X-ray spectroscopy (EDS, Fig. 4c-e) confirmed overall high-fidelity of the backfilling process and that mesostructural ordering was maintained from the monolithic template to the final nanocomposite. Compared with bulk In metal in the form of a foil of similar thickness to the monolithic composite, In confined to nanoscale dimensions in the GD template showed dramatically different superconducting properties. Temperature-dependent measurements of the magnetic properties revealed a higher T_c (~3.7 K), attributed to modified electron-phonon coupling (phonon softening) [47], and a much broader transition until saturation, attributed to confinement effects (quantum size effects) opposing phonon softening in superconductors (Fig. 4f). Furthermore, measurements at constant temperature below T_c (i.e., 2 K) showed a substantial increase of the critical magnetic field (B_c) at which the superconducting state is destroyed (from about 30 mT to 0.83 T), and that effectively the behavior had switched from a type-I to a type-II superconductor (Fig. 4g). This could be rationalized by a substantial reduction of the

Cooper pair coherence length from 360 nm in bulk In to about 20 nm in the backfilled mesostructure, consistent with the thickness of the G^D minority network struts occupied by the In metal. These results suggested that the BCP directed mesoscale structure is dictating macroscopic behavior via modifications of fundamental, quantum level characteristics of the superconducting materials. They further illustrated the significant academic/fundamental interest in these novel soft-matter self-assembly based approaches to quantum materials.

2.3. BCP self-assembly-directed superconducting thin films

Among numerous applications envisioned for superconductors, electronic devices employing superconducting components are long sought after thanks to their power efficiency and applications in quantum information science, among others [51]. To that end, thin film form factors of BCP self-assembly-directed superconductors are of particular interest. In turn, this is contingent upon their ability to be incorporated into thin-film nanofabrication processes that underpin modern integrated circuit manufacturing. Earlier results were based on EISA of BCP-niobia solutions which yielded free-standing films with thickness up to a millimeter and shapes determined by the geometry of the evaporation container. Capitalizing on the solution processability of BCP self-assembly directed materials, in recent experiments of the Wiesner

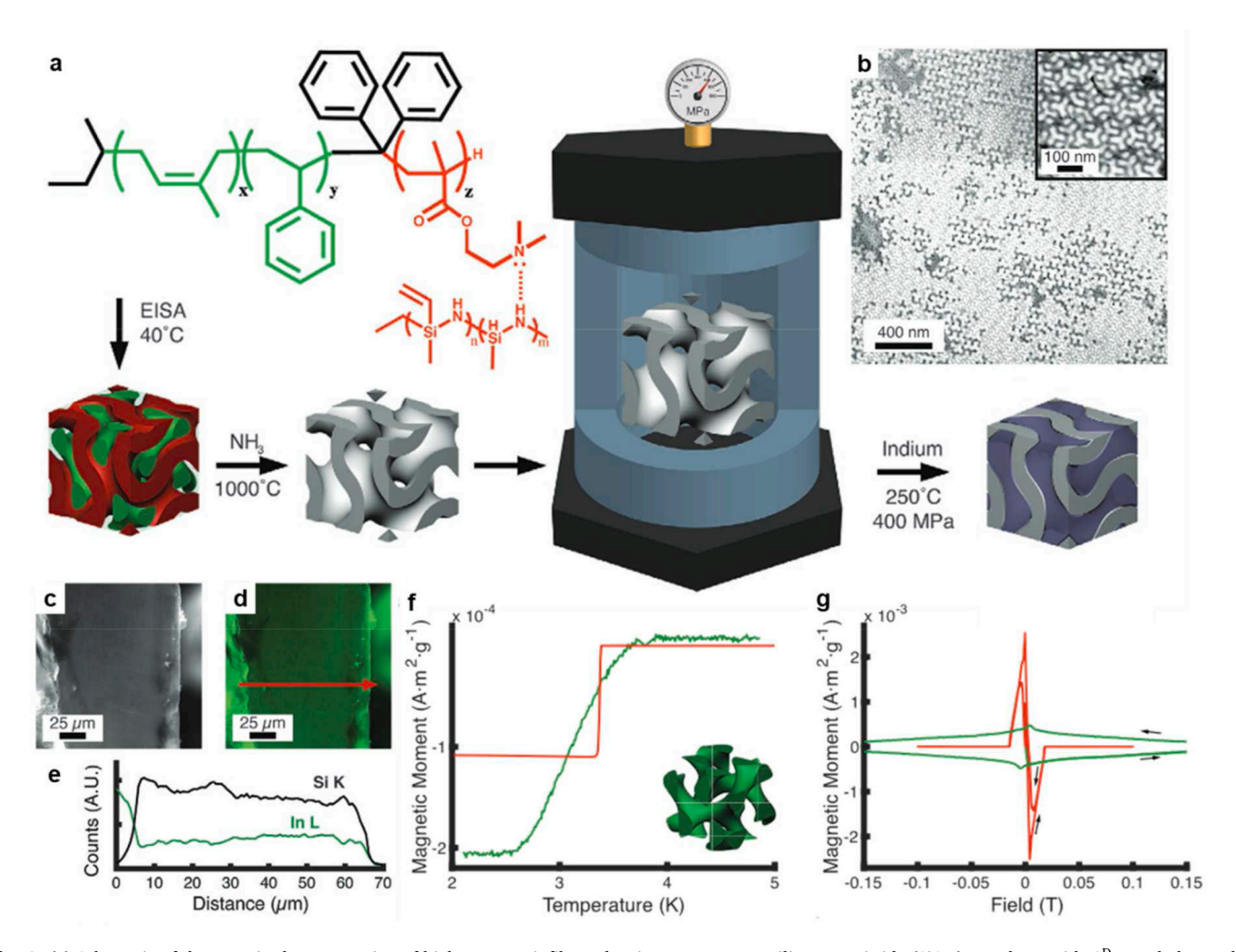


Fig. 4. (a) Schematic of the steps in the preparation of high-pressure infiltrated In into mesoporous silicon oxynitride (SiON) templates with G^D morphology self-assembled from triblock terpolymer PI-b-PS-b-PDMAEMA (ISA) through EISA in toluene. (b) SEM image of In/SiON composite showing In with brighter contrast resulting from the higher backscattered electron signal (inset: higher magnification image revealing a signature morphology for gyroidal structures). (c) SEM image at low magnification of the cross section of a monolith of the backfilled In/SiON composite. (d) In elemental mapping (in green) measured by energy-dispersive spectroscopy (EDS) superimposed on the same area shown in (c). (e) X-ray photon counts from In (green) and Si (black) along the red arrow in (d). (f) Temperature-dependent and (g) external-field-dependent magnetic moments, the latter measured at 2 K, of the In/SiON composite (green) and an In foil (red) with similar thickness as the composite monolith. Inset in (f) depicts the In as a set of two interpenetrating (but never touching) gyroidal minority networks after infiltration. Arrows in (g) indicate scanning direction of the external field. Adapted from Ref. [46] with permission. © 2021 Wiley-VCH.

group, ISO-niobia solutions were simply spin-coated on a single-crystal silicon (Si) wafer substrate creating supported thin films with thickness below 1 μ m that could be transformed into mesoporous superconducting NbCN thin films after further heat treatments in various gas environments as described in earlier sections (Fig. 5a–e) [50]. Due to rapid solvent evaporation during spin-coating, resulting thin film morphologies as probed by SEM and grazing incidence SAXS (GISAXS) could be best described as G^A structures compressed along their film normal direction (Fig. 51-n). Heat treatments generated inorganic materials with a cubic rock salt structure as evidenced by grazing incidence wide-angle X-ray scattering (GIWAXS, Fig. 50), consistent with NbN or NbCN (vide supra).

Low-temperature transport measurements on such thin films revealed a T_c of 12.8 K (Fig. 5p). Interestingly, above T_c , an exponential rise in resistivity with decreasing temperature was consistent with an Arrhenius-like activation barrier, shedding light on the granular nature of NbCN superconducting thin films in a tortuous gyroidal network morphology. Furthermore, extrapolation of field-dependent T_c values suggested an upper critical field (B_{c2}) of the spin-coated NbCN thin films of 16.6 T (Fig. 5q). This exceeds literature values reported for bulk NbCN materials and is another testament of how BCP self-assembly directed

synthesis approaches can produce high quality quantum materials with unexpected behavior. Granular superconductors constitute an interesting research topic in their own right [52], and further experiments will have to show how such structural features of BCP self-assembly directed quantum materials may give rise to advanced materials properties.

Finally, as a proof of principle, before conversion to the desired NbN or NbCN materials, the as made BCP-niobia sol hybrid thin films were shown to be compatible with (photo)lithographic patterning approaches (Fig. 5f–k), creating hierarchically ordered thin film structures on both the nano- and microscales (Fig. 5r). Superconductivity was observed of a NbCN strip derived in this way and subsequent thermal processing, albeit with a lower T_c (Fig. 5s). The emergent technology of photolithographically patterning a superconducting film derived from spincoating a BCP-niobia sol solution not only expands the form factors available to solution derived self-assembled quantum materials, but also encourages further integration into microelectronic fabrication to realize their full academic and technological potential.

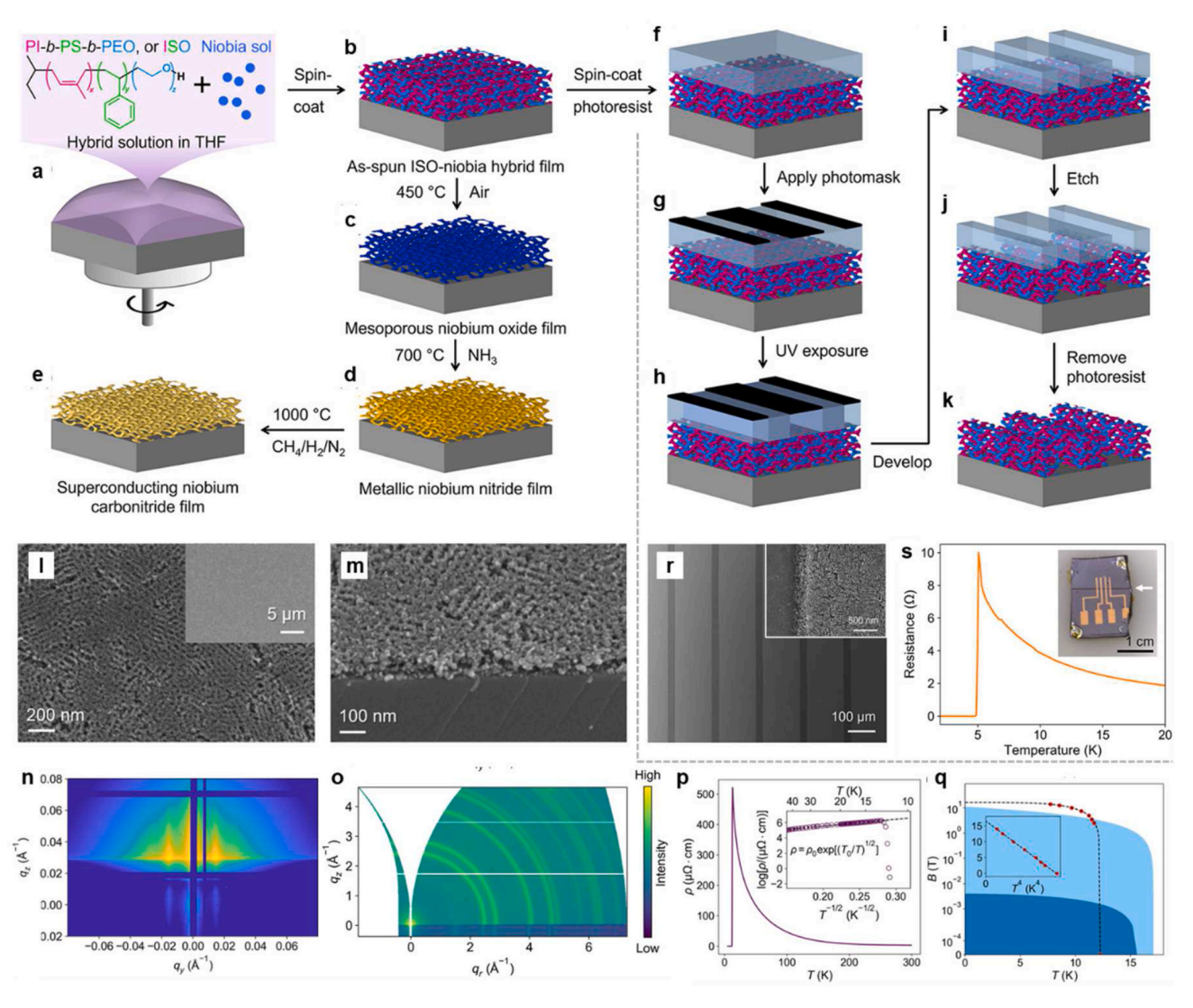


Fig. 5. (a–e) Schematic of the procedure to prepare mesoporous superconducting NbCN thin films by spin-coating ISO-niobia solutions and subsequent heat treatments in various gas environments. (f–k) Schematic of lithographic procedures to define patterns of as-made BCP self-assembly directed niobia-sol nanoparticle composite thin films, which can subsequently be converted to superconducting materials via steps shown in (c–e). (l) Plan view and (m) 45° tilt view SEM images of BCP directed NbCN thin films. Inset in (l) shows a smooth, crack-free film at low magnification. Two dimensional (n) grazing incidence small-angle X-ray scattering (GISAXS) and (o) grazing incidence wide-angle X-ray scattering (GIWAXS) patterns of BCP directed NbCN thin films. (p) Plot of resistivity (ρ) as a function of temperature (T) of a BCP directed NbCN thin film measured using the van der Pauw method. Inset shows a fit to the plot of the logarithm of ρ as a function of $T^{-1/2}$. (q) Plot of upper critical field (B_{c2}) as a function of T. Dark and light blue regions depict the pure superconducting and mixed states, respectively, in the phase diagram of bulk NbN/NbCN superconductors (data from Refs. [48,49]). (r) SEM image of BCP directed NbCN thin films patterned by photolithography, with etched strips shown in dark. Inset shows the area near the patterned strip edge at higher magnification. (s) Plot of resistance of a single patterned NbCN strip as a function of temperature. Inset shows a photo of a single lithographically patterned NbCN strip (400 μm wide, pointed to by the white arrow) with four colinear metal contacts across the strip used for the transport measurements. Note that the NbCN strip shows up as a darker line against the background in this optical microscope image. Adapted from Ref. [50] with permission. © 2021 American Chemical Society.

2.4. Superconducting asymmetric structures via non-equilibrium processes of BCP self-assembly

Up to this point, we have reviewed BCP self-assembly-directed superconductors with uniform, narrowly-distributed pore sizes. Equilibrium morphologies are achieved, e.g., by slow solvent evaporation during EISA or by solvent vapor annealing for thin films after spin-coating. Moving to non-equilibrium processes of BCP self-assembly could provide access, e.g., to novel asymmetric structures with interesting properties and applications for superconducting quantum materials. One such process combines BCP self-assembly with industrially proven and scalable non-solvent induced phase separation (NIPS) [53, 54]. The combination is referred to as SNIPS (NIPS + SA) [55] and proceeds by casting and partially evaporating a BCP solution on a

substrate followed by plunging the sample into a non-solvent bath (typically water). Precipitation induced by the non-solvent converts the concentration gradient along the film normal from incomplete evaporation into a pore gradient. The resulting non-equilibrated $\sim\!100$ nm thick mesoporous top separation layer is periodically ordered from BCP self-assembly. The support structure of $\sim\!100$ µm thickness has a hierarchical pore structure with a gradient of mesopores from the top all the way to macropores at the bottom with either sponge-like or finger-like morphologies [56]. When triblock terpolymers are used in SNIPS, the entire support structure also has mesopores everywhere, including in the macroporous walls. Such asymmetric and hierarchical membrane structures not only combine high selectivity and permeability substantially enhancing liquid separation processes [57], they also are interesting for electrochemical energy devices, e.g., for energy conversion

and storage applications, as they simultaneously provide high surface area and rapid transport [58].

Non-equilibrium processes like the BCP self-assembly directed SNIPS process can also structure direct inorganic materials, similar to what has been described in previous sections. In this way, carbon, titania (TiO₂), and titanium nitride (TiN) materials with asymmetric and hierarchical pore structures were obtained after calcination of the as-made SNIPS derived hybrids obtained from poly(isoprene-block-styrene-block-4vinylpyridine) (ISV) as structure directing agents for carbon and titania precursors [59,60]. Carbon and TiN materials with hierarchically ordered asymmetric pore structures and mesopores everywhere combined high surface area with rapid transport resulting in extraordinary performance, e.g., as electrochemical double-layer capacitors [58]. After nitridation under ammonia at higher temperatures of the titania precursor derived materials, employing thermal processes described earlier, the resulting titanium nitride (TiN) membranes exhibited a finger-like morphology of the asymmetric substructure (Fig. 6b) with a homogenous mesoporous top separation layer (Fig. 6c-d). The bottom was open with macropores (Fig. 6f) and showed mesopores everywhere, including in the walls of the macropores (Fig. 6g). The coarsened grains seen in SEM images were a consequence of the propensity for both TiO₂ and TiN to crystallize at a lower temperature than their niobium counterparts [60]. XRD profiles were consistent with a cubic phase of TiN (Fig. 6h). Conductivity decreased with increasing temperature, displaying metallic behavior (Fig. 6i). Finally, asymmetric TiN (a type-II superconductor) exhibited the Meissner effect with an onset T_c of 3.8 K (Fig. 6j). Such superconducting membranes could be useful for separation based on magnetism [61]. Although further studies are needed to explore what emergent superconducting behavior may arise from asymmetric structures, non-equilibrium processes such as SNIPS certainly add to the toolbox for the formation of BCP self-assembly-directed quantum materials.

3. Other quantum materials via BCP self-assembly

3.1. Topological materials enabled by self-assembled BCP mesostructures

With its origin traced back to the quantum Hall effect [62], topological materials are a category of quantum materials that also have gained significant attention in recent years. A complete and rigorous introduction to this abstract topic is beyond the scope of this perspective article, and readers are referred to existing reviews in the literature [18]. Suffices to say here that it is helpful to bear in mind that, within the framework of topological materials, different phases of matter can not only be classified by their symmetry, but also by the topology of their band structures [18]. The "topology of band structures" refers to the fact that a topological index (also known as topological invariant) can mathematically be defined and computed to characterize its topological order (as opposed to the order solely imposed by symmetry). Materials with different topologies of their band structures have different topological indices, which only takes on discreet integer values. For example, a materials system may be tweaked through perturbations in the form of an external field or strain, causing a corresponding change in its electronic band structure, but its topological phase as determined by the topological index may remain the same.

The majority of the theoretical and experimental work on topological materials in condensed matter physics is concerned with identification of materials with topologically nontrivial electronic states, such as 2D topological insulators [65,66] that have a conducting surface while the inside/bulk of the material is non-conducting. Precise electronic band structure engineering is required during experimental materials synthesis for topological phenomena to emerge, which obviously poses a problem when organic materials such as non-conducting polymers are involved. Since topology is embedded in the band structure, it extends to non-electronic band structures as well, including those describing photonic and phononic behavior of periodically ordered structures. BCPs are

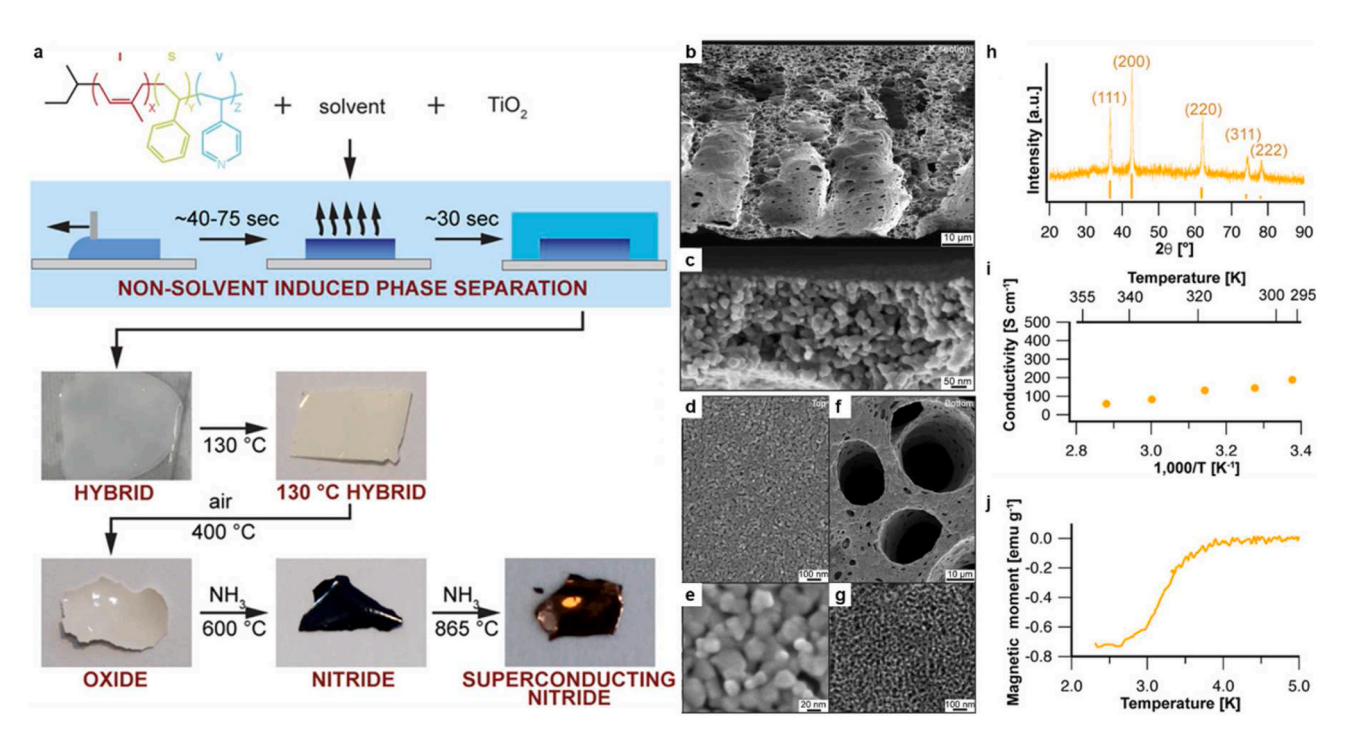


Fig. 6. (a) Schematic of the procedure to prepare superconducting asymmetric membrane structures via BCP self-assembly combined with non-solvent induced phase separation (SNIPS) and subsequent heat treatment in air and NH₃. The casting hybrid solution consists of poly(isoprene-block-styrene-block-4-vinylpyridine) (ISV) and TiO₂ sol nanoparticles. SEM images of (b) the asymmetric cross section, (c) the mesoporous cross section near the top surface, (d,e) mesoporous top surface at different magnifications, (f) macroporous bottom surface, and (g) mesoporous pore wall of the final TiN. (h) XRD profile of asymmetric TiN structure. Ticks indicate expected peak positions and relative peak intensities for cubic TiN from PDF 00-038-1420. (i) Temperature-dependent conductivity of an asymmetric TiN structure exhibiting metallic behavior. (j) Temperature-dependent magnetic moment of a superconducting asymmetric TiN structure. Adapted from Ref. [58] with permission. © 2021 American Chemical Society.

known to self-assemble into mesostructures that have been theoretically predicted to possess intriguing photonic as well as phononic properties, including negative refraction [67] and complete photonic and phononic band gaps [68,69]. In a computational study it was recently shown that reducing point group symmetry from the \boldsymbol{G}^D (\boldsymbol{O}_h symmetry) across the \boldsymbol{G}^A (O symmetry) to a deformed \boldsymbol{G}^A structure (\boldsymbol{D}_2 symmetry) provides general symmetry constraints enabling access to topologically protected Weyl points in 3D photonic and phononic crystals [64]. A Weyl point is a topological feature that manifests itself as two linearly crossing bands in the band structure of a material (Fig. 7k,l). This study therefore provided a roadmap how to design self-assembly based materials to experimentally realize such topological quantum materials in block copolymer self-assembly based materials.

To that end, the Wiesner group prepared thin films of mesoporous resin/carbon in the form of a G^A network by spin-coating a hybrid solution of ISO and resorcinol resols (carbon precursor) and subsequent solvent vapor annealing and pyrolysis (Fig. 7a–f) [70]. To increase the refractive index contrast, amorphous Si was backfilled into the resin/carbon template and crystallized through laser induced nanosecond-scale transient heating and melting [71]. The crystalline Si took on the inverse structure of the template that was eventually removed by piranha etching (Fig. 7g–i). Careful analysis of the GISAXS pattern of the final crystalline Si with the template etched away revealed that the symmetry was reduced to D₂ (or space group F222, Fig. 7j) [63], the exact same symmetry constraint for which the existence of Weyl points in the photonic/phononic band structure of such materials had

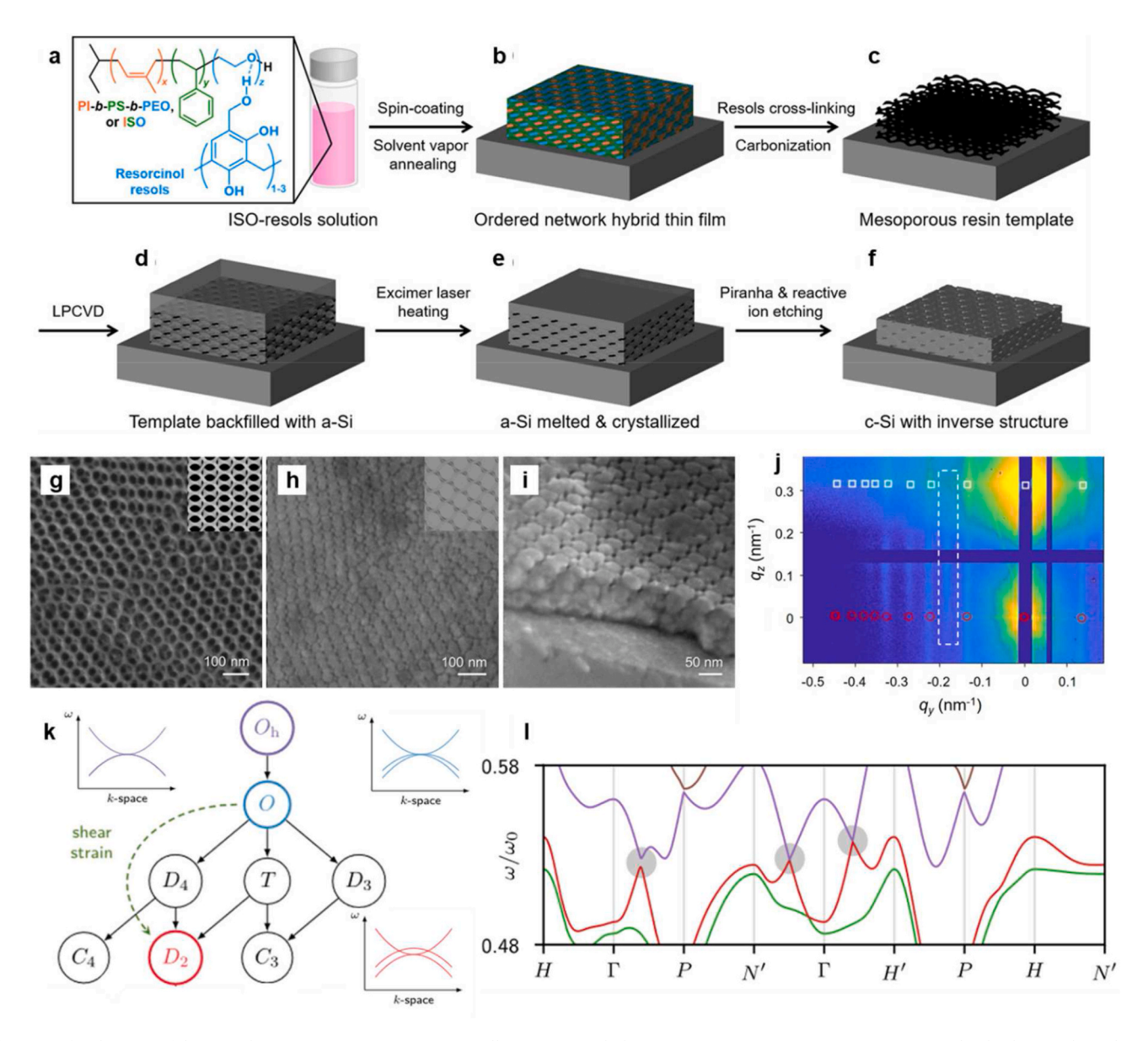


Fig. 7. (a–f) Schematic of the procedure to prepare mesoporous crystalline Si (cSi) with the necessary D_2 point group symmetry expected to lead to topological Weyl points. Mesoporous resin/carbon thin-film template is first fabricated using ISO as structure directing agent with the PEO block swelled by resorcinol resols as carbon precursor. Conversion to a mesoporous carbon by heating under non-oxidizing conditions allows backfilling this template with amorphous Si (aSi) via low-pressure chemical vapor deposition (LPCVD). Transient laser heating of this composite in air preserves the structural integrity of the carbon template while crystallizing the Si (aSi to cSi transition) deposited into the template. SEM images of (g) resin/carbon template and (h,i) templated crystalline Si (top view and side view) after template removal. (j) Select area of two dimensional GISAXS pattern of the final mesostructured Si, showing an additional reflection in the dashed rectangle not consistent with the G^A symmetry, whose expected reflections are labeled with white squares and red circles. (k) Point group symmetry reduction from G^D (O_h), through G^A (O), to deformed G^A (D₂). Corresponding (schematic) band structures show band crossing in D₂. (l) Computed photonic band structures of deformed G^A : Weyl points occur along Γ -N' and Γ -H'. Adapted from Refs. [63,64] with permission. © 2020 American Chemical Society.

been predicted (vide supra). While the existence of Weyl points was not demonstrated in this paper, the results pointed to a roadmap from solution-based BCP self-assembly toward topological quantum materials.

3.2. Complex magnets using BCPs as structure directing agents

Complex magnets are another type of quantum materials attracting increasing research attention. Arising from the spin magnetic moment, materials magnetism is intrinsically quantum based, and mesostructured magnets via BCP self-assembly have been reported in the literature, such as superparamagnetic γ-iron oxide (γ-Fe₂O₃) particles embedded in aluminosilicate walls structure directed by poly(isoprene-block-ethylene oxide) (PI-b-PEO) [72]. On top of the three classical categories of dia-, para-, and ferromagnetic materials, the coupled ferromagnetism and ferroelectricity in multiferroic materials allow for the manipulation of magnetization via electric polarization or vice versa, which is of fundamental interest to the study of spintronics, or spin electronics, e.g., for next-generation quantum computers. The microphase segregation in BCP self-assembly enables the construction of coexisting ferromagnetic and ferroelectric components in the self-assembled structure, e.g., by incorporating respective precursors into either the hydrophilic or the hydrophobic block of amphiphilic BCPs, giving rise to a nanocomposite of ferromagnetic and ferroelectric materials after the removal of the BCP

In another example, single-phase multiferroic bismuth ferrite (BiFeO₃) was structure directed by an amphiphilic BCP as a thin film on a Si substrate (Fig. 8a and b) [74]. Higher calcination temperatures led to what the authors called "disorder" films exhibiting a mesostructure of crystalline BiFeO₃ but without long-range periodic order (Fig. 8c). Compared to a non-porous dense reference material the disorder film of mesoporous BiFeO₃ displayed greatly enhanced susceptibility (dM/dH) as well as saturation magnetization upon the application of an external

electric field (Fig. 8d,f). Interestingly, distinct anisotropic behavior was observed for the susceptibility, but not for the saturation magnetization (Fig. 8f and g). The dominant mechanism at play was the enhanced spin canting in the nanostructure, together with a second mechanism of changed magnetocrystalline anisotropy that favored the perpendicular orientation. This was closely related to strain built up during the solution-based film formation and the subsequent thermal treatment. It is worth noting, that such strain engineering was accomplished without the use of the exquisite MBE technique.

4. Outlook and conclusion

Quantum materials are a fast-growing and fascinating field that has garnered world-wide attention in science and engineering communities as well as with the public. BCP self-assembly-directed quantum materials add an entirely new facet to this rapidly advancing field. Despite recent progress summarized in this perspective article, substantial opportunities as well as challenges lie ahead for future investigations to realize the full academic and technological potential of such hybrid approaches.

Underlying the often exotic properties demonstrated by quantum materials is their electronic structure, e.g., the energy gap described in the BCS theory of superconductivity [17] or the surface states in topological insulators [18]. Obtaining a clear fundamental understanding of the detailed electronic structure of quantum materials has been a persistent driver of new discoveries in this field. State-of-the-art techniques for probing band structures such as angle-resolved photoemission spectroscopy (ARPES) [75] require single crystalline samples, however. With only a few notable exceptions [45,76,77], single crystals of either the mesostructured lattice or the inorganic atomic lattice are a rare find in mesostructured inorganic materials processed via wet chemical soft matter approaches. Notwithstanding its own distinctive effects on quantum behavior [52], the granular nature of BCP self-assembly

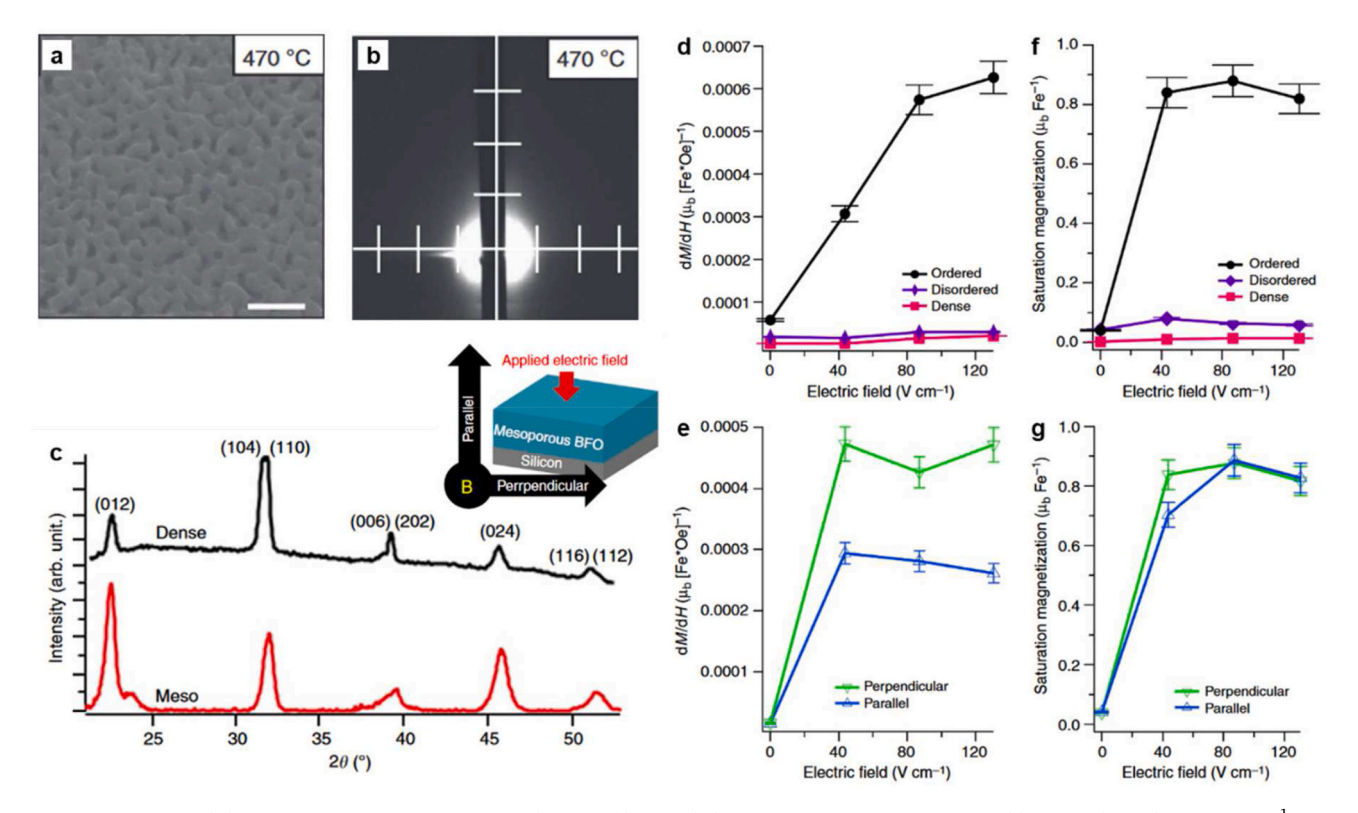


Fig. 8. (a) SEM image and (b) GISAXS pattern of mesostructured BiFeO $_3$ films. Scale bar in (a) represents 100 nm. Neighboring ticks in (b) are 0.2 nm^{-1} apart. (c) XRD profile of a mesostructured BiFeO $_3$ film in comparison with a dense film. The inset shows the orientation of electric and magnet fields used in (d–g). Plots of (d,e) magnetic susceptibility and (f,g) saturation magnetization as a function of applied electric field. Comparisons are plotted between (d,f) mesostructured, disordered, and dense films and (e,g) different magnetization orientations. Adapted from Ref. [74] with permission. © 2015 Springer Nature.

directed NbN superconductors described earlier complicates a serious inquiry into the electronic structure of such quantum materials. Nanosecond transient laser heating has been successful in generating single crystalline inorganic materials in templates from BCP self-assembly under extreme non-equilibrium conditions [76], yet at the time the mesostructure was not yet periodically ordered to even approach a single crystal state. While in subsequent studies periodically ordered templates were used in similar experiments, in turn the resulting inorganic materials were not a single crystal [10,63,71,78]. Considering that the constituent carbon atoms are arranged in a single crystalline sheet in magic-angle graphene, where a superlattice of larger periodicities surprisingly induces superconductivity [23], or that an artificial charge modulation is enabled by single crystalline films interfaced in superlattices [79], it is of critical importance for future studies to explore methods to realize "single crystals in single crystals". This would include, e.g., single crystalline inorganic materials remaining in registry throughout a single-crystal mesostructural porous gyroidal network as described in this article (vide supra).

Self-assembled mesoporous structures directed by BCP self-assembly have large surface areas, a coveted feature, e.g., for applications in energy storage and conversion systems [14] like capacitors [58] or 3D batteries [80], or as catalyst supports [81]. Such large surface area materials should also provide a fruitful playground for the investigation of interfacial phenomena in quantum materials, but to date this remains largely unexplored. Superconductivity appeared when two insulating oxides, lanthanum aluminate (LaAlO₃) and strontium titanate (SrTiO₃), were interfaced [82], and the T_c was boosted from only 9 K in bulk iron selenide (FeSe) to 65 K when a monolayer FeSe was deposited on SrTiO₃ [83,84]. Interfacial engineering in BCP self-assembly-directed quantum materials pretty much remains an uncharted territory, partly due to the requirement of epitaxy between materials structures and the challenges associated with acquiring single crystals in self-assembled mesostructures (vide supra). Still, as a first step, a general backfilling approach could be devised to interface two or more materials to study possible emergent behavior.

Back to BCP self-assembly itself, two thrusts may guide its convergence with quantum materials and unleash its full potential. On the one hand, new self-assembled structures and their formation pathways are far from being exhausted and await discovery. The history of cubic cocontinuous network mesophases based on minimal surfaces [85-87] reminds us of the seemingly unlimited possibilities afforded by BCP self-assembly [88], some of which already have been, and in the future undoubtably will further be, connected to novel quantum material discoveries. Hexagonally arranged chiral helices allowed light to propagate without backscattering on the surface [89], equivalent to the photonic version of a topological insulator. In fact, such helical structures on the mesoscale derived from BCP self-assembly have already been reported [90,91]. Besides new mesophases, symmetry breaking of known structures through mesoscale lattice deformations, similar to epitaxial strain engineering in thin film atomic single crystals [92,93], may result in unexpected behavior as well, e.g., as described here by compression of an alternating gyroid structure predicted to lead to topologically protected Weyl points in photonic and phononic band structures [63]. Efforts are clearly needed to grow mesoscale single crystals [45] to facilitate characterization and fundamental understanding, similar to atomic single crystal counterparts (vide supra). On the other hand, BCP self-assembly can be the assistive tool for device fabrication involving quantum materials, particularly in the thin film regime. Ultimately, to be applied in a device, quantum materials need to be patterned by lithography and integrated onto chips. Lithographic techniques using BCP self-assembly are attractive for the small pitch size enabled by short, strongly segregating blocks with a large Flory-Huggins parameter (χ) [94] and the defect-free array of BCP domains with long-range order [95,96]. Last but not least, laser annealing can be employed for aligning mesostructures, pattern definition, and/or physical/chemical conversion of quantum materials [78,97].

In conclusion, the combination of BCP self-assembly and quantum materials represents an emerging and promising research field for polymer science in particular, and materials science in general, that will provide complementary synergy to both fields. "Soft" organic BCPs, with their high tunability and solution processability, have already enabled synthesis of a series of "hard" inorganic quantum materials with unique mesostructures and unconventional properties. By converging these otherwise divergent fields, the scientific merit spurs the prospect of manipulating quantum phenomena through the formation of periodically ordered mesoscopic structures, while the technological promise relies on reliable and scalable synthesis approaches that evade traditional quantum materials formation techniques. To gain better fundamental understanding of BCP self-assembly-directed quantum materials, materials quality has to be improved, structural control perfected, and processing conditions refined. Large volume reconstruction techniques to visualize BCP defects and grain boundaries in unprecedented ways have recently come online, and promise substantially improved understanding [98]. Continued research efforts at the interface of such soft matter crystals with crystalline atomic systems holds the promise of revolutionizing quantum materials research by discovering tantalizing (and maybe perplexing) materials behavior.

Declaration of competing interest

The authors declare the following financial interests/personal relationships which may be considered as potential competing interests: Ulrich Wiesner reports financial support was provided by National Science Foundation. Ulrich Wiesner reports financial support was provided by US Department of Energy. Ulrich Wiesner has patent pending to Cornell University.

Data availability

No data was used for the research described in the article.

Acknowledgements

U.W. would like to thank the National Science Foundation (NSF) Single Investigator Award (DMR-1707836) as well as the U.S. Department of Energy (DOE), Office of Science, Basic Energy Sciences (DE-SC0010560) for funding of different aspects of this work.

References

- N.A. Zaidi, S.R. Giblin, I. Terry, A.P. Monkman, Room temperature magnetic order in an organic magnet derived from polyaniline, Polymer 45 (2004) 5683–5689, https://doi.org/10.1016/j.polymer.2004.06.002.
- [2] C. Paquet, E. Kumacheva, Nanostructured polymers for photonics, Mater. Today 11 (2008) 48–56, https://doi.org/10.1016/\$1369-7021(08)70056-7.
- [3] F.S. Bates, G.H. Fredrickson, Block copolymer thermodynamics: theory and experiment, Annu. Rev. Phys. Chem. 41 (1990) 525–557, https://doi.org/10.1146/ annurev.physchem.41.1.525.
- [4] K. Hur, U. Wiesner, Design and applications of multiscale organic-inorganic hybrid materials derived from block copolymer self-assembly, in: V. Percec (Ed.), Hierarchical Macromol. Struct. 60 Years Staudinger Nobel Prize II, Springer International Publishing, Cham, 2013, https://doi.org/10.1007/978-3-319-03719-6
- [5] T.N. Hoheisel, K. Hur, U.B. Wiesner, Block copolymer-nanoparticle hybrid selfassembly, Prog. Polym. Sci. 40 (2015) 3–32, https://doi.org/10.1016/j. progpolymsci.2014.10.002.
- [6] M. Templin, A. Franck, A.D. Chesne, H. Leist, Y. Zhang, R. Ulrich, V. Schädler, U. Wiesner, Organically modified aluminosilicate mesostructures from block copolymer phases, Science 278 (1997) 1795–1798, https://doi.org/10.1126/ science 278 5344 1795
- [7] C. Liang, K. Hong, G.A. Guiochon, J.W. Mays, S. Dai, Synthesis of a large-scale highly ordered porous carbon film by self-assembly of block copolymers, Angew. Chem. Int. Ed. 43 (2004) 5785–5789, https://doi.org/10.1002/anie.200461051.
- [8] J.G. Werner, T.N. Hoheisel, U. Wiesner, Synthesis and characterization of gyroidal mesoporous carbons and carbon monoliths with tunable ultralarge pore size, ACS Nano 8 (2014) 731–743, https://doi.org/10.1021/nn405392t.

- [9] M. Kamperman, C.B.W. Garcia, P. Du, H. Ow, U. Wiesner, Ordered mesoporous ceramics stable up to 1500 °C from diblock copolymer mesophases, J. Am. Chem. Soc. 126 (2004) 14708–14709, https://doi.org/10.1021/ja046795h.
- [10] K.W. Tan, B. Jung, J.G. Werner, E.R. Rhoades, M.O. Thompson, U. Wiesner, Transient laser heating induced hierarchical porous structures from block copolymer–directed self-assembly, Science 349 (2015) 54–58, https://doi.org/ 10.1126/science.aab0492.
- [11] S.C. Warren, L.C. Messina, L.S. Slaughter, M. Kamperman, Q. Zhou, S.M. Gruner, F. J. DiSalvo, U. Wiesner, Ordered mesoporous materials from metal nanoparticle-block copolymer self-assembly, Science 320 (2008) 1748–1752, https://doi.org/10.1126/science.1159950.
- [12] P. Yang, D. Zhao, D.I. Margolese, B.F. Chmelka, G.D. Stucky, Generalized syntheses of large-pore mesoporous metal oxides with semicrystalline frameworks, Nature 396 (1998) 152–155, https://doi.org/10.1038/24132.
- [13] J. Lee, M. Christopher Orilall, S.C. Warren, M. Kamperman, F.J. DiSalvo, U. Wiesner, Direct access to thermally stable and highly crystalline mesoporous transition-metal oxides with uniform pores, Nat. Mater. 7 (2008) 222–228, https://doi.org/10.1038/nmat2111.
- [14] C. Li, Q. Li, Y.V. Kaneti, D. Hou, Y. Yamauchi, Y. Mai, Self-assembly of block copolymers towards mesoporous materials for energy storage and conversion systems, Chem. Soc. Rev. 49 (2020) 4681–4736, https://doi.org/10.1039/ DOCS000216
- [15] R.P. Thedford, F. Yu, W.R.T. Tait, K. Shastri, F. Monticone, U. Wiesner, The promise of soft-matter-enabled quantum materials, Adv. Mater. 35 (2023), 2203908, https://doi.org/10.1002/adma.202203908.
- [16] R. Cava, N. de Leon, W. Xie, Introduction: quantum materials, Chem. Rev. 121 (2021) 2777–2779, https://doi.org/10.1021/acs.chemrev.0c01322.
- [17] M. Tinkham, Introduction to Superconductivity, second ed., Courier Corporation, 2004
- [18] M.Z. Hasan, C.L. Kane, Colloquium: topological insulators, Rev. Mod. Phys. 82 (2010) 3045–3067, https://doi.org/10.1103/RevModPhys.82.3045.
- [19] C. Nisoli, R. Moessner, P. Schiffer, Colloquium: artificial spin ice: designing and imaging magnetic frustration, Rev. Mod. Phys. 85 (2013) 1473–1490, https://doi. org/10.1103/RevModPhys.85.1473.
- [20] Y. Zhou, K. Kanoda, T.-K. Ng, Quantum spin liquid states, Rev. Mod. Phys. 89 (2017), 025003, https://doi.org/10.1103/RevModPhys.89.025003.
- [21] M.A. Nielsen, I.L. Chuang, Quantum Computation and Quantum Information, 10th anniversary ed, Cambridge University Press, Cambridge; New York, 2010.
- [22] F. Arute, K. Arya, R. Babbush, D. Bacon, J.C. Bardin, R. Barends, R. Biswas, S. Boixo, F.G.S.L. Brandao, D.A. Buell, B. Burkett, Y. Chen, Z. Chen, B. Chiaro, R. Collins, W. Courtney, A. Dunsworth, E. Farhi, B. Foxen, A. Fowler, C. Gidney, M. Giustina, R. Graff, K. Guerin, S. Habegger, M.P. Harrigan, M.J. Hartmann, A. Ho, M. Hoffmann, T. Huang, T.S. Humble, S.V. Isakov, E. Jeffrey, Z. Jiang, D. Kafri, K. Kechedzhi, J. Kelly, P.V. Klimov, S. Knysh, A. Korotkov, F. Kostritsa, D. Landhuis, M. Lindmark, E. Lucero, D. Lyakh, S. Mandrà, J.R. McClean, M. McEwen, A. Megrant, X. Mi, K. Michielsen, M. Mohseni, J. Mutus, O. Naaman, M. Neeley, C. Neill, M.Y. Niu, E. Ostby, A. Petukhov, J.C. Platt, C. Quintana, E. G. Rieffel, P. Roushan, N.C. Rubin, D. Sank, K.J. Satzinger, V. Smelyanskiy, K. J. Sung, M.D. Trevithick, A. Vainsencher, B. Villalonga, T. White, Z.J. Yao, P. Yeh, A. Zalcman, H. Neven, J.M. Martinis, Quantum supremacy using a programmable superconducting processor, Nature 574 (2019) 505–510, https://doi.org/10.1038/s41586-019-1666-5.
- [23] Y. Cao, V. Fatemi, S. Fang, K. Watanabe, T. Taniguchi, E. Kaxiras, P. Jarillo-Herrero, Unconventional superconductivity in magic-angle graphene superlattices, Nature 556 (2018) 43–50, https://doi.org/10.1038/nature26160.
- [24] B.A. Joyce, Molecular beam epitaxy, Rep. Prog. Phys. 48 (1985) 1637–1697.
- [25] D.B. Chrisey, G.K. Hubler (Eds.), Pulsed Laser Deposition of Thin Films, John Wiley & Sons, Hoboken, 1994.
- [26] R.L. Truby, J.A. Lewis, Printing soft matter in three dimensions, Nature 540 (2016) 371–378, https://doi.org/10.1038/nature21003.
- [27] A.N. Semenov, Contribution to the theory of microphase layering in block-copolymer melts, Sov. Phys. JETP 61 (1985) 733–742.
- [28] G. Polymeropoulos, G. Zapsas, K. Ntetsikas, P. Bilalis, Y. Gnanou, N. Hadjichristidis, 50th anniversary perspective: polymers with complex architectures, Macromolecules 50 (2017) 1253–1290, https://doi.org/10.1021/ acs.macromol.6b02569.
- [29] J. Unsworth, J. Du, B.J. Crosby, P. Bryant, YBa₂Cu₃O_{7-x} superconducting ceramic/ thermoplastic 0–3 composites, Mater. Res. Bull. 26 (1991) 1041–1050.
- [30] H.-Y. Hsueh, Y.-C. Huang, R.-M. Ho, C.-H. Lai, T. Makida, H. Hasegawa, Nanoporous gyroid nickel from block copolymer templates via electroless plating, Adv. Mater. 23 (2011) 3041–3046, https://doi.org/10.1002/adma.201100883.
- [31] J. Kao, P. Bai, J.M. Lucas, A.P. Alivisatos, T. Xu, Size-dependent assemblies of nanoparticle mixtures in thin films, J. Am. Chem. Soc. 135 (2013) 1680–1683, https://doi.org/10.1021/ja3107912.
- [32] J. Fan, S.W. Boettcher, G.D. Stucky, Nanoparticle assembly of ordered multicomponent mesostructured metal oxides via a versatile Sol—Gel process, Chem. Mater. 18 (2006) 6391–6396, https://doi.org/10.1021/cm062359d.
- [33] S.W. Robbins, P.A. Beaucage, H. Sai, K.W. Tan, J.G. Werner, J.P. Sethna, F. J. DiSalvo, S.M. Gruner, R.B. Van Dover, U. Wiesner, Block copolymer self-assembly-directed synthesis of mesoporous gyroidal superconductors, Sci. Adv. 2 (2016), e1501119, https://doi.org/10.1126/sciadv.1501119.
- [34] G.N. Gol'tsman, O. Okunev, G. Chulkova, A. Lipatov, A. Semenov, K. Smirnov, B. Voronov, A. Dzardanov, C. Williams, R. Sobolewski, Picosecond superconducting single-photon optical detector, Appl. Phys. Lett. 79 (2001) 705–707, https://doi.org/10.1063/1.1388868.

[35] H. Yamamori, M. Ishizaki, A. Shoji, P.D. Dresselhaus, S.P. Benz, 10V programmable Josephson voltage standard circuits using NbN/TiNx/NbN/TiNx/NbN doublejunction stacks, Appl. Phys. Lett. 88 (2006), 042503, https://doi.org/10.1063/ 1.216.7780

- [36] R. Baskaran, A.V. Thanikai Arasu, E.P. Amaladass, M.P. Janawadkar, High upper critical field in disordered niobium nitride superconductor, J. Appl. Phys. 116 (2014), 163908, https://doi.org/10.1063/1.4900436.
- [37] S.C. Warren, F.J. DiSalvo, U. Wiesner, Nanoparticle-tuned assembly and disassembly of mesostructured silica hybrids, Nat. Mater. 6 (2007) 156–161, https://doi.org/10.1038/nmat1819.
- [38] W. Meissner, R. Ochsenfeld, Ein neuer Effekt bei Eintritt der Supraleitfähigkeit, Naturwissenschaften 21 (1933) 787–788.
- [39] H. Rögener, Zur Supraleitung des Niobnitrids, Z. Phys. 132 (1952) 446-467.
- [40] J.R. Gavaler, M.A. Janocko, J.K. Hulm, C.K. Jones, Superconducting properties as a function of thickness in NbN films, Physica 55 (1971) 585–591.
- [41] G. Oya, Y. Onodera, Transition temperatures and crystal structures of single-crystal and polycrystalline NbN x films, J. Appl. Phys. 45 (1974) 1389–1397, https://doi. org/10.1063/1.1663418.
- [42] P.W. Anderson, Theory of dirty superconductors, J. Phys. Chem. Solid. 11 (1959)
- [43] P.A. Beaucage, R.B. van Dover, F.J. DiSalvo, S.M. Gruner, U. Wiesner, Superconducting quantum metamaterials from convergence of soft and hard condensed matter science, Adv. Mater. 33 (2021), 2006975, https://doi.org/ 10.1002/adma.202006975.
- [44] E.M. Susca, P.A. Beaucage, M.A. Hanson, U. Werner-Zwanziger, J.W. Zwanziger, L. A. Estroff, U. Wiesner, Self-assembled gyroidal mesoporous polymer-derived high temperature ceramic monoliths, Chem. Mater. 28 (2016) 2131–2137, https://doi.org/10.1021/acs.chemmater.5b05011.
- [45] E.M. Susca, P.A. Beaucage, R.P. Thedford, A. Singer, S.M. Gruner, L.A. Estroff, U. Wiesner, Preparation of macroscopic block-copolymer-based gyroidal mesoscale single crystals by solvent evaporation, Adv. Mater. 31 (2019), 1902565, https://doi.org/10.1002/adma.201902565.
- [46] R.P. Thedford, P.A. Beaucage, E.M. Susca, C.A. Chao, K.C. Nowack, R.B. Van Dover, S.M. Gruner, U. Wiesner, Superconducting quantum metamaterials from high pressure melt infiltration of metals into block copolymer double gyroid derived ceramic templates, Adv. Funct. Mater. 31 (2021), 2100469, https://doi. org/10.1002/adfm.202100469.
- [47] W.L. McMillan, Transition temperature of strong-coupled superconductors, Phys. Rev. 167 (1968) 331–344, https://doi.org/10.1103/PhysRev.167.331.
- [48] M.P. Mathur, D.W. Deis, J.R. Gavaler, Lower critical field measurements in NbN bulk and thin films, J. Appl. Phys. 43 (1972) 3158–3161, https://doi.org/10.1063/ 1.1661678.
- [49] M.J. Raine, D.P. Hampshire, Characterization of the low temperature superconductor niobium carbonitride, IEEE Trans. Appl. Supercond. 21 (2011) 3138–3141. https://doi.org/10.1109/TASC.2010.2095491.
- [50] F. Yu, R.P. Thedford, K.R. Hedderick, G. Freychet, M. Zhernenkov, L.A. Estroff, K. C. Nowack, S.M. Gruner, U.B. Wiesner, Patternable mesoporous thin film quantum materials via block copolymer self-assembly: an emergent technology? ACS Appl. Mater. Interfaces 13 (2021) 34732–34741, https://doi.org/10.1021/acsami_1c09085
- [51] M.H. Devoret, R.J. Schoelkopf, Superconducting circuits for quantum information: an outlook, Science 339 (2013) 1169–1174, https://doi.org/10.1126/ science.1231930.
- [52] G. Deutscher, Granular superconductivity: a playground for Josephson, anderson, kondo, and mott, J. Supercond. Nov. Magnetism 34 (2021) 1699–1703, https:// doi.org/10.1007/s10948-020-05773-y.
- [53] K.-V. Peinemann, V. Abetz, P.F.W. Simon, Asymmetric superstructure formed in a block copolymer via phase separation, Nat. Mater. 6 (2007) 992–996, https://doi. org/10.1038/nmat2038.
- [54] W.A. Phillip, R.M. Dorin, J. Werner, E.M.V. Hoek, U. Wiesner, M. Elimelech, Tuning structure and properties of graded triblock terpolymer-based mesoporous and hybrid films, Nano Lett. 11 (2011) 2892–2900, https://doi.org/10.1021/ nl2013554.
- [55] R.M. Dorin, D.S. Marques, H. Sai, U. Vainio, W.A. Phillip, K.-V. Peinemann, S. P. Nunes, U. Wiesner, Solution small-angle X-ray scattering as a screening and predictive tool in the fabrication of asymmetric block copolymer membranes, ACS Macro Lett. 1 (2012) 614–617, https://doi.org/10.1021/mz300100b.
- [56] Q. Zhang, Y.M. Li, Y. Gu, R.M. Dorin, U. Wiesner, Tuning substructure and properties of supported asymmetric triblock terpolymer membranes, Polymer 107 (2016) 398–405, https://doi.org/10.1016/j.polymer.2016.07.076.
- [57] M.M. Pendergast, R. Mika Dorin, W.A. Phillip, U. Wiesner, E.M.V. Hoek, Understanding the structure and performance of self-assembled triblock terpolymer membranes, J. Membr. Sci. 444 (2013) 461–468, https://doi.org/ 10.1016/j.memsci.2013.04.074.
- [58] S.A. Hesse, K.E. Fritz, P.A. Beaucage, R.P. Thedford, F. Yu, F.J. DiSalvo, J. Suntivich, U. Wiesner, Materials combining asymmetric pore structures with well-defined mesoporosity for energy storage and conversion, ACS Nano 14 (2020) 16897–16906, https://doi.org/10.1021/acsnano.0c05903.
- [59] S.A. Hesse, P.A. Beaucage, D.-M. Smilgies, U. Wiesner, Structurally asymmetric porous carbon materials with ordered top surface layers from nonequilibrium block copolymer self-assembly, Macromolecules 54 (2021) 2979–2991, https://doi.org/ 10.1021/acs.macromol.0c02720.
- [60] S.A. Hesse, K.E. Fritz, P.A. Beaucage, E.M. Susca, J. Suntivich, U. Wiesner, Oxides and nitrides with asymmetric pore structure from block copolymer Co-assembly and non-solvent induced phase separation, Macromol. Chem. Phys. 224 (2023), 2200304, https://doi.org/10.1002/macp.202200304.

- [61] E.-S. Jang, J.-J. Chang, J. Gwak, A. Ayral, V. Rouessac, L. Cot, S.-J. Hwang, J.-H. Choy, Asymmetric high- T c superconducting gas separation membrane, Chem. Mater. 19 (2007) 3840–3844, https://doi.org/10.1021/cm070656s.
- [62] K.v. Klitzing, G. Dorda, M. Pepper, New method for high-accuracy determination of the fine-structure constant based on quantized Hall resistance, Phys. Rev. Lett. 45 (1980) 494–497, https://doi.org/10.1103/PhysRevLett.45.494.
- [63] F. Yu, Q. Zhang, R.P. Thedford, A. Singer, D.-M. Smilgies, M.O. Thompson, U. B. Wiesner, Block copolymer self-assembly-directed and transient laser heating-enabled nanostructures toward phononic and photonic quantum materials, ACS Nano 14 (2020) 11273–11282, https://doi.org/10.1021/acsnano.0c03150.
- [64] M. Fruchart, S.-Y. Jeon, K. Hur, V. Cheianov, U. Wiesner, V. Vitelli, Soft self-assembly of Weyl materials for light and sound, Proc. Natl. Acad. Sci. USA 115 (2018) E3655–E3664, https://doi.org/10.1073/pnas.1720828115.
- [65] B.A. Bernevig, T.L. Hughes, S.-C. Zhang, Quantum spin Hall effect and topological phase transition in HgTe quantum wells, Science 314 (2006) 1757–1761, https:// doi.org/10.7551/mitpress/8053.003.0075.
- [66] M. König, S. Wiedmann, C. Brüne, A. Roth, H. Buhmann, L.W. Molenkamp, X.-L. Qi, S.-C. Zhang, Quantum spin Hall insulator state in HgTe quantum wells, Science 318 (2007) 766–770, https://doi.org/10.1126/science.1148047.
- [67] K. Hur, Y. Francescato, V. Giannini, S.A. Maier, R.G. Hennig, U. Wiesner, Three-dimensionally isotropic negative refractive index materials from block copolymer self-assembled chiral gyroid networks, Angew. Chem. Int. Ed. 50 (2011) 11985–11989, https://doi.org/10.1002/anie.201104888.
- [68] A.C. Edrington, A.M. Urbas, P. DeRege, C.X. Chen, T.M. Swager, N. Hadjichristidis, M. Xenidou, L.J. Fetters, J.D. Joannopoulos, Y. Fink, E.L. Thomas, Polymer-based photonic crystals, Adv. Mater. 13 (2001) 421–425.
- [69] K. Hur, R.G. Hennig, U. Wiesner, Exploring periodic bicontinuous cubic network structures with complete phononic bandgaps, J. Phys. Chem. C 121 (2017) 22347–22352, https://doi.org/10.1021/acs.jpcc.7b07267.
- [70] Q. Zhang, F. Matsuoka, H.S. Suh, P.A. Beaucage, S. Xiong, D.-M. Smilgies, K. W. Tan, J.G. Werner, P.F. Nealey, U.B. Wiesner, Pathways to mesoporous resin/carbon thin films with alternating gyroid morphology, ACS Nano 12 (2018) 347–358, https://doi.org/10.1021/acsnano.7b06436.
- [71] K.W. Tan, J.G. Werner, M.D. Goodman, H.S. Kim, B. Jung, H. Sai, P.V. Braun, M. O. Thompson, U. Wiesner, Synthesis and formation mechanism of all-organic block copolymer-directed templating of laser-induced crystalline silicon nanostructures, ACS Appl. Mater. Interfaces 10 (2018) 42777–42785, https://doi.org/10.1021/acsgmi.8b1.706
- [72] C. Garcia, Y. Zhang, F. DiSalvo, U. Wiesner, Mesoporous aluminosilicate materials with superparamagnetic γ-Fe2O3 particles embedded in the walls, Angew. Chem. Int. Ed. 42 (2003) 1526–1530, https://doi.org/10.1002/anie.200250618.
- [73] S. Ren, R.M. Briber, M. Wuttig, Diblock copolymer based self-assembled nanomagnetoelectric, Appl. Phys. Lett. 93 (2008), 173507, https://doi.org/ 10.1063/1.3005558.
- [74] T.E. Quickel, L.T. Schelhas, R.A. Farrell, N. Petkov, V.H. Le, S.H. Tolbert, Mesoporous bismuth ferrite with amplified magnetoelectric coupling and electric field-induced ferrimagnetism, Nat. Commun. 6 (2015) 6562, https://doi.org/ 10.1038/ncomms/7562
- [75] H. Zhang, T. Pincelli, C. Jozwiak, T. Kondo, R. Ernstorfer, T. Sato, S. Zhou, Angleresolved photoemission spectroscopy, Nat. Rev. Methods Primer. 2 (2022) 54, https://doi.org/10.1038/s43586-022-00133-7.
- [76] H. Arora, P. Du, K.W. Tan, J.K. Hyun, J. Grazul, H.L. Xin, D.A. Muller, M. O. Thompson, U. Wiesner, Block copolymer self-assembly-directed single-crystal homo- and heteroepitaxial nanostructures, Science 330 (2010) 214–219, https://doi.org/10.1126/science.1193369.
- [77] E.J.W. Crossland, N. Noel, V. Sivaram, T. Leijtens, J.A. Alexander-Webber, H. J. Snaith, Mesoporous TiO2 single crystals delivering enhanced mobility and optoelectronic device performance, Nature 495 (2013) 215–219, https://doi.org/10.1038/nature11936.
- [78] K.W. Tan, U. Wiesner, Block copolymer self-assembly directed hierarchically structured materials from nonequilibrium transient laser heating, Macromolecules 52 (2019) 395–409, https://doi.org/10.1021/acs.macromol.8b01766.
- [79] A. Ohtomo, D.A. Muller, J.L. Grazul, H.Y. Hwang, Artificial charge-modulationin atomic-scale perovskite titanate superlattices, Nature 419 (2002) 378–380, https://doi.org/10.1038/nature00977.
- [80] J.G. Werner, G.G. Rodríguez-Calero, H.D. Abruña, U. Wiesner, Block copolymer derived 3-D interpenetrating multifunctional gyroidal nanohybrids for electrical energy storage, Energy Environ. Sci. 11 (2018) 1261–1270, https://doi.org/ 10.1039/C7EE03571C.

- [81] K.E. Fritz, P.A. Beaucage, F. Matsuoka, U. Wiesner, J. Suntivich, Mesoporous titanium and niobium nitrides as conductive and stable electrocatalyst supports in acid environments, Chem. Commun. 53 (2017) 7250–7253, https://doi.org/ 10.1039/C7C03232C
- [82] N. Reyren, S. Thiel, A.D. Caviglia, L.F. Kourkoutis, G. Hammerl, C. Richter, C. W. Schneider, T. Kopp, A.-S. Rüetschi, D. Jaccard, M. Gabay, D.A. Muller, J.-M. Triscone, J. Mannhart, Superconducting interfaces between insulating oxides, Science 317 (2007) 1196–1199, https://doi.org/10.1126/science.1146006.
- [83] Q.-Y. Wang, Z. Li, W.-H. Zhang, Z.-C. Zhang, J.-S. Zhang, W. Li, H. Ding, Y.-B. Ou, P. Deng, K. Chang, J. Wen, C.-L. Song, K. He, J.-F. Jia, S.-H. Ji, Y.-Y. Wang, L.-L. Wang, X. Chen, X.-C. Ma, Q.-K. Xue, Interface-induced high-temperature superconductivity in single unit-cell FeSe films on SrTiO 3, chin, Phys. Lett. 29 (2012), 037402, https://doi.org/10.1088/0256-307X/29/3/037402.
- [84] S. He, J. He, W. Zhang, L. Zhao, D. Liu, X. Liu, D. Mou, Y.-B. Ou, Q.-Y. Wang, Z. Li, L. Wang, Y. Peng, Y. Liu, C. Chen, L. Yu, G. Liu, X. Dong, J. Zhang, C. Chen, Z. Xu, X. Chen, X. Ma, Q. Xue, X.J. Zhou, Phase diagram and electronic indication of high-temperature superconductivity at 65 K in single-layer FeSe films, Nat. Mater. 12 (2013) 605–610, https://doi.org/10.1038/mmat3648.
- [85] E.L. Thomas, D.B. Alward, D.J. Kinning, D.C. Martin, D.L. Handlin, L.J. Fetters, Ordered bicontinuous double-diamond structure of star block copolymers: a new equilibrium microdomain morphology, Macromolecules 19 (1986) 2197–2202, https://doi.org/10.1021/ma00162a016.
- [86] D.A. Hajduk, P.E. Harper, S.M. Gruner, C.C. Honeker, G. Kim, E.L. Thomas, L. J. Fetters, The gyroid: a new equilibrium morphology in weakly segregated diblock copolymers, Macromolecules 27 (1994) 4063–4075, https://doi.org/10.1021/ms00933006
- [87] A. Jain, G.E.S. Toombes, L.M. Hall, S. Mahajan, C.B.W. Garcia, W. Probst, S. M. Gruner, U. Wiesner, Direct access to bicontinuous skeletal inorganic plumber's nightmare networks from block copolymers, Angew. Chem. Int. Ed. 44 (2005) 1226–1229, https://doi.org/10.1002/anie.200461156.
- [88] F.S. Bates, M.A. Hillmyer, T.P. Lodge, C.M. Bates, K.T. Delaney, G.H. Fredrickson, Multiblock polymers: panacea or pandora's box? Science 336 (2012) 434–440, https://doi.org/10.1126/science.1215368.
- [89] M.C. Rechtsman, J.M. Zeuner, Y. Plotnik, Y. Lumer, D. Podolsky, F. Dreisow, S. Nolte, M. Segev, A. Szameit, Photonic Floquet topological insulators, Nature 496 (2013) 196–200, https://doi.org/10.1038/nature12066.
- [90] U. Krappe, R. Stadler, I. Voigt-Martin, Chiral assembly in amorphous ABC triblock copolymers. Formation of a helical morphology in polystyrene-blockpolybutadiene-block-poly(methyl methacrylate) block copolymers, Macromolecules 28 (1995) 4558–4561. https://doi.org/10.1021/ma00117a027.
- [91] R.-M. Ho, Y.-W. Chiang, C.-K. Chen, H.-W. Wang, H. Hasegawa, S. Akasaka, E. L. Thomas, C. Burger, B.S. Hsiao, Block copolymers with a twist, J. Am. Chem. Soc. 131 (2009) 18533–18542, https://doi.org/10.1021/ja9083804.
 [92] J.H. Haeni, P. Irvin, W. Chang, R. Uecker, P. Reiche, Y.L. Li, S. Choudhury, W. Tian,
- [92] J.H. Haeni, P. Irvin, W. Chang, R. Uecker, P. Reiche, Y.L. Li, S. Choudhury, W. Tian, M.E. Hawley, B. Craigo, A.K. Tagantsev, X.Q. Pan, S.K. Streiffer, L.Q. Chen, S. W. Kirchoefer, J. Levy, D.G. Schlom, Room-temperature ferroelectricity in strained SrTiO₃, Nature 430 (2004) 758–761.
- [93] D.G. Schlom, L.-Q. Chen, C.-B. Eom, K.M. Rabe, S.K. Streiffer, J.-M. Triscone, Strain tuning of ferroelectric thin films, Annu. Rev. Mater. Res. 37 (2007) 589–626, https://doi.org/10.1146/annurey.matsci.37.061206.113016.
- [94] C. Sinturel, F.S. Bates, M.A. Hillmyer, High χ-low N block polymers: how far can we go? ACS Macro Lett. 4 (2015) 1044–1050, https://doi.org/10.1021/ acsmacrolett 5b00472
- [95] R. Ruiz, H. Kang, F.A. Detcheverry, E. Dobisz, D.S. Kercher, T.R. Albrecht, J.J. D. Pablo, P.F. Nealey, Density multiplication and improved lithography by directed copolymer assembly, Science 321 (2008) 936–939, https://doi.org/10.1126/ science.1157626.
- [96] I. Bita, J.K.W. Yang, Y.Y. Jung, C.A. Ross, E.L. Thomas, K.K. Berggren, Graphoepitaxy of self-assembled block copolymers on two-dimensional periodic patterned templates, Science 321 (2008) 939–943.
- [97] P. W. Majewski, A. Rahman, C.T. Black, K.G. Yager, Arbitrary lattice symmetries via block copolymer nanomeshes, Nat. Commun. 6 (2015) 7448, https://doi.org/ 10.1038/ncomms8448
- [98] X. Feng, C.J. Burke, M. Zhuo, H. Guo, K. Yang, A. Reddy, I. Prasad, R.-M. Ho, A. Avgeropoulos, G.M. Grason, E.L. Thomas, Seeing mesoatomic distortions in softmatter crystals of a double-gyroid block copolymer, Nature 575 (2019) 175–179, https://doi.org/10.1038/s41586-019-1706-1.